Electronic Supplementary Material (ESI) for Chemical Science.
This journal is © The Royal Society of Chemistry 2019

Supplementary Electronic Information

On the Unsuspected Role of Multivalent Metal Ions on the Charge Storage of a Metal Oxide Electrode in Mild Aqueous Electrolytes

Yee-Seul Kim,[a] Kenneth D. Harris,[b,c] Benoît Limoges,*[,a] Véronique Balland*[,a]

[a] Université de Paris, Laboratoire d'Electrochimie Moléculaire UMR 7591, CNRS, F-75013 Paris, France
[b] Nanotechnology Research Institute, National Research Council Canada, Edmonton, Alberta T6G 2M9, Canada
[c] Department of Mechanical Engineering, University of Alberta, Edmonton, Alberta T6G 2V4, Canada

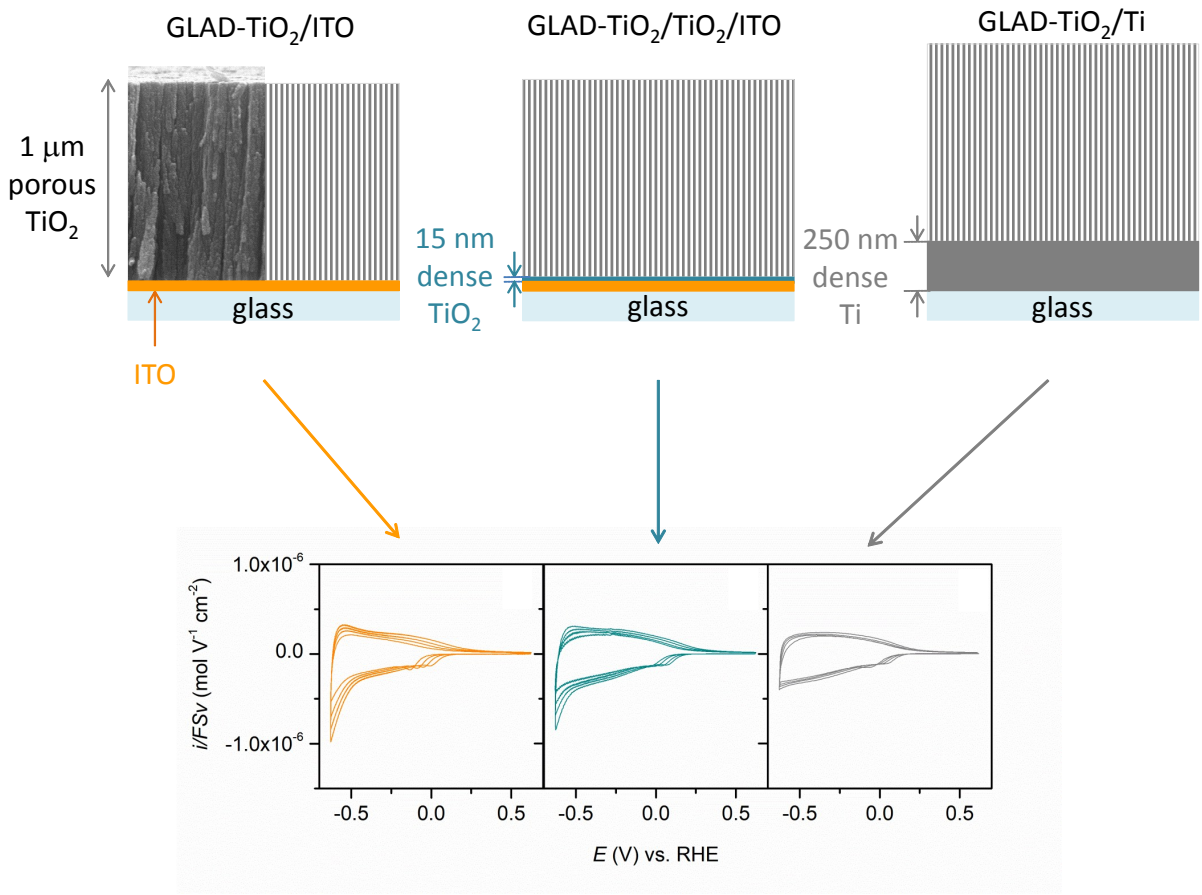

Figure S1. (Top) Schematic representations of the 1-µm thick mesoporous GLAD-TiO_2 electrodes used in the present study and previous work, including (top, left) GLAD-TiO_2/ITO from previous work[S1], (top, center) GLAD-TiO_2/TiO_2/ITO and (top, right) GLAD/TiO_2/Ti. (Bottom) Cyclic voltammograms (normalized to the scan rate and geometric surface area) corresponding to the electrodes above recorded at different scan rates *v* (ranging from 0.05 to 0.5 V s^{-1}) in an aqueous electrolyte containing 0.3 M KCl (pH > 5).

Comments. In our previous work,[S1] the mesoporous GLAD-TiO_2 film was directly deposited on a ITO substrate, leaving a fraction of the underlying ITO surface accessible to the aqueous electrolyte *via* the film porosity. The main problem with this electrode configuration was the electrochemical instability of the unprotected ITO surface, which under strongly reducing conditions (*i.e.*, upon applying exceedingly negative potentials for prolonged time) led to irreversible reduction with a complete loss of the electrical properties.[S2] In order to avoid/minimize this electrode failure and to allow for the application of exceedingly negative potentials, we prepared two new types of GLAD-TiO_2 electrode architectures. First, a structure in which the ITO surface was isolated from the aqueous electrolyte by a thin compact layer of TiO_2 (15-nm, generated in the GLAD evaporator using a non-glancing deposition angle of 0°) over which the 1-µm thick mesoporous GLAD-TiO_2 film was then deposited (at a glancing deposition angle of 72°). For the second electrode structure, the underlying conductive ITO layer was completely replaced with a metallic titanium layer (250 nm thickness) over which the 1-µm thick mesoporous GLAD-TiO_2 film was deposited (at a deposition angle of 72°).

The main advantage of the GLAD-TiO_2/TiO_2/ITO electrodes over the GLAD-TiO_2/Ti electrodes is that they remain optically transparent in the UV-visible region, which is useful for spectroelectrochemical studies. Moreover, the presence of the thin layer of dense TiO_2 does not significantly alter the electrochemical response (Figure S1). As anticipated, the electrochemical stability of the GLAD-TiO_2/TiO_2/ITO electrodes was significantly improved compare to our previous GLAD-TiO_2/ ITO electrodes when they were polarized at highly negative potentials. However, under prolonged and strongly reducing conditions they were still irreversibly degraded, an effect we have attributed to the presence of defects and/or pinholes in the bulk TiO_2 coating that impedes a definitive protection of the ITO surface from the aqueous electrolyte. In contrast, with the GLAD-TiO_2/Ti electrodes it was possible to apply strongly reducing conductions without electrode failure, clearly demonstrating that the electrode failure was the result of the electrochemical instability of the underlying conductive ITO material under strongly reducing potentials.

The morphology of the mesoporous GLAD-TiO_2 film is not expected to strongly depend on the nature of the underlying substrate. In order to confirm that the GLAD-TiO_2 films, once deposited under identical conditions, behave similarly whatever the substrate used, the different GLAD-TiO_2 electrodes were characterized by CV in an aqueous electrolyte containing no insertion cations, *i.e.* in 0.3 M KCl electrolyte of pH > 5 (Figure S1). Under these conditions, the great similarities observed between CVs recorded with each of the three different types of GLAD-TiO_2 electrodes (Figure S1) suggest no significant difference in the double layer charging capacitance (especially at potentials below 0 V *vs.* RHE where TiO_2 behaves as a metal-like conductive material). From this, we conclude that all of these mesoporous semiconductive films possess similar surface area enhancement and porosity. It can be noticed that at potential below –0.5 V *vs.* RHE, the GLAD-TiO_2/ITO and GLAD-TiO_2/TiO_2/ITO electrodes show, on their forward cathodic scans in CV, the rise of a faradaic current response, characteristic of an irreversible reduction of the underlying ITO substrate, an electrochemical process that is not present in the CVs of the GLAD-TiO_2/Ti electrode. This result is in line with our assumption of ITO instability under strongly reducing conditions.

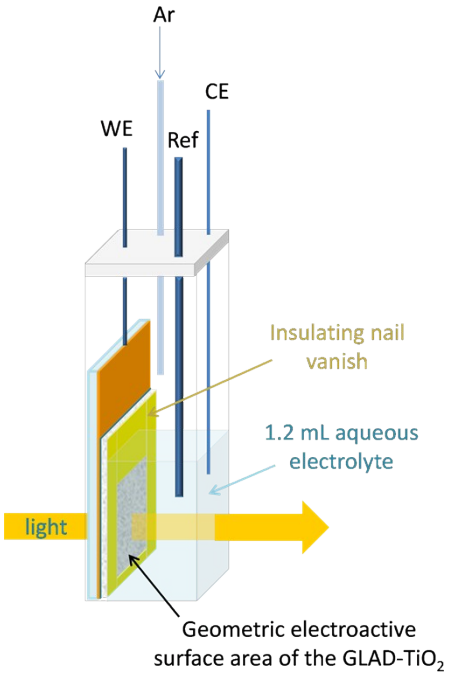

Figure S2. Schematic representation of the three-electrode spectroelectrochemical cell (1-cm optical path length) used in the present study to investigate the charge storage at GLAD-TiO_2/TiO_2/ITO electrodes. The geometric electrode surface area (~0.5 cm^2) is delimited by nail vanish. Electrical contact with the working electrodes is made at the top of the electrode at a location where the underlying ITO/glass substrate was not coated with GLAD-TiO_2/TiO_2. The electrolyte volume was ca. 1.2 mL. Prior to electrochemical measurements, the electrolyte was thoroughly degassed by argon bubbling. The counter electrode was a Pt wire, and the reference electrode an Ag/AgCl/sat. KCl (+0.2 V *vs.* NHE).

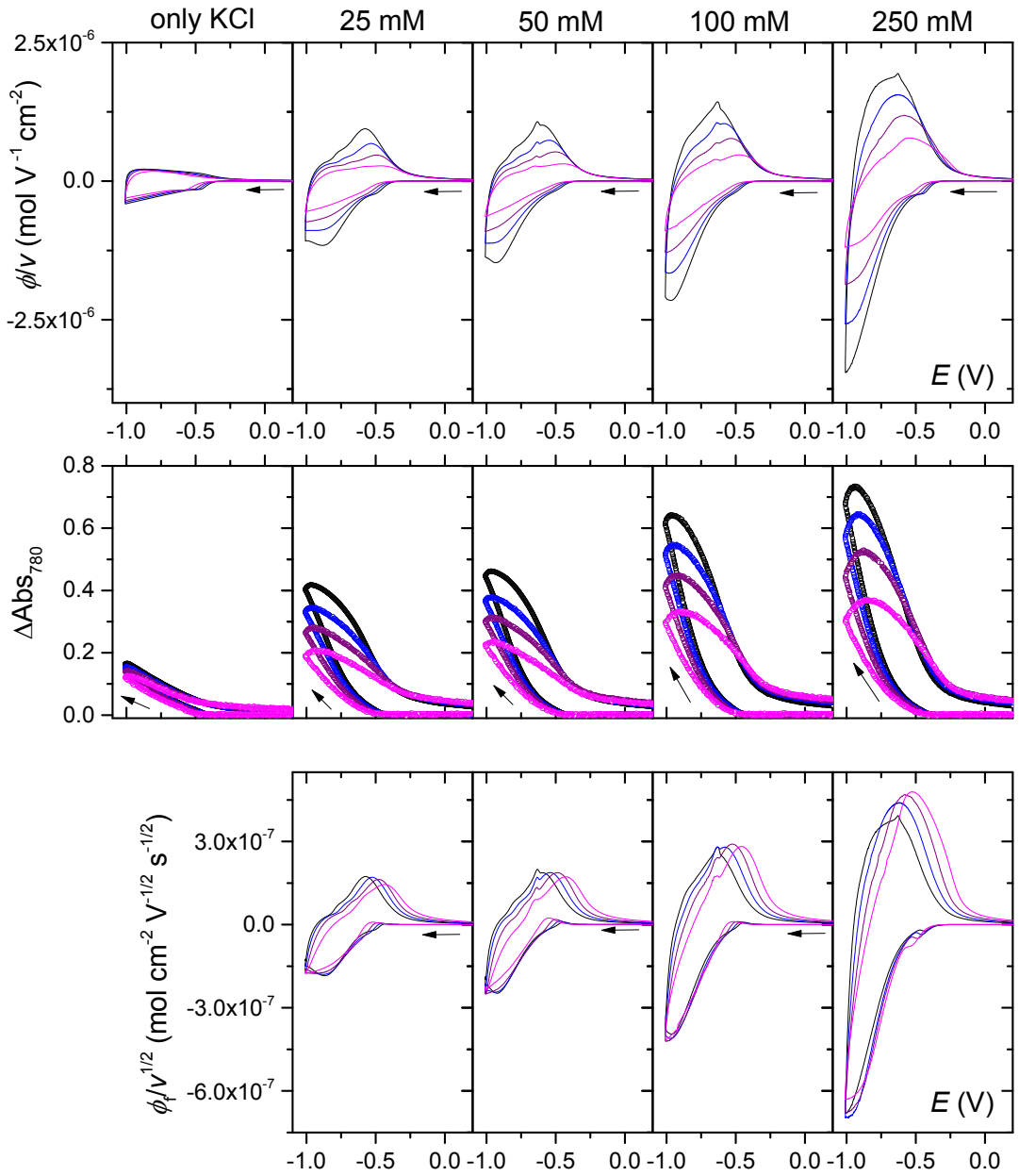

Figure S3. (Top) Cyclic voltammograms and (middle) cyclic voltabsorptograms (at 780 nm) recorded at a GLAD-TiO_2/TiO_2/ITO electrode in different aqueous electrolyte solutions (adjusted to pH 3.0) containing 0.3 M KCl and increasing concentrations of $AlCl_3$ (from left to right: 0, 25, 50, 100 mM), or (last right graph) without KCl and only 250 mM $AlCl_3$ (the KCl and $AlCl_3$ concentrations are also reported on top of the figure). Currents are converted to flux density normalised to the scan rate. The scan rate was (black) 50, (blue) 100, (violet) 250, and (magenta) 500 mV·s^{-1}. (Bottom) Faradaic current component (corrected from the capacitive current) expressed in flux density and normalized to the square root of the scan rate.

On bottom graphs, the fact that the CV responses normalized to $v^{1/2}$ are nearly overlaid whatever the scan rate suggests that the reversible faradaic process is a diffusion-controlled process. Moreover, the magnitude of the cathodic or anodic peak current is linearly increased with the concentration of $AlCl_3$ (see also the inset of Figure 5 in the article) which indicates that the process is rate-controlled by the diffusional mass transport of $[Al(H_2O)_6]^{3+}$ in solution.

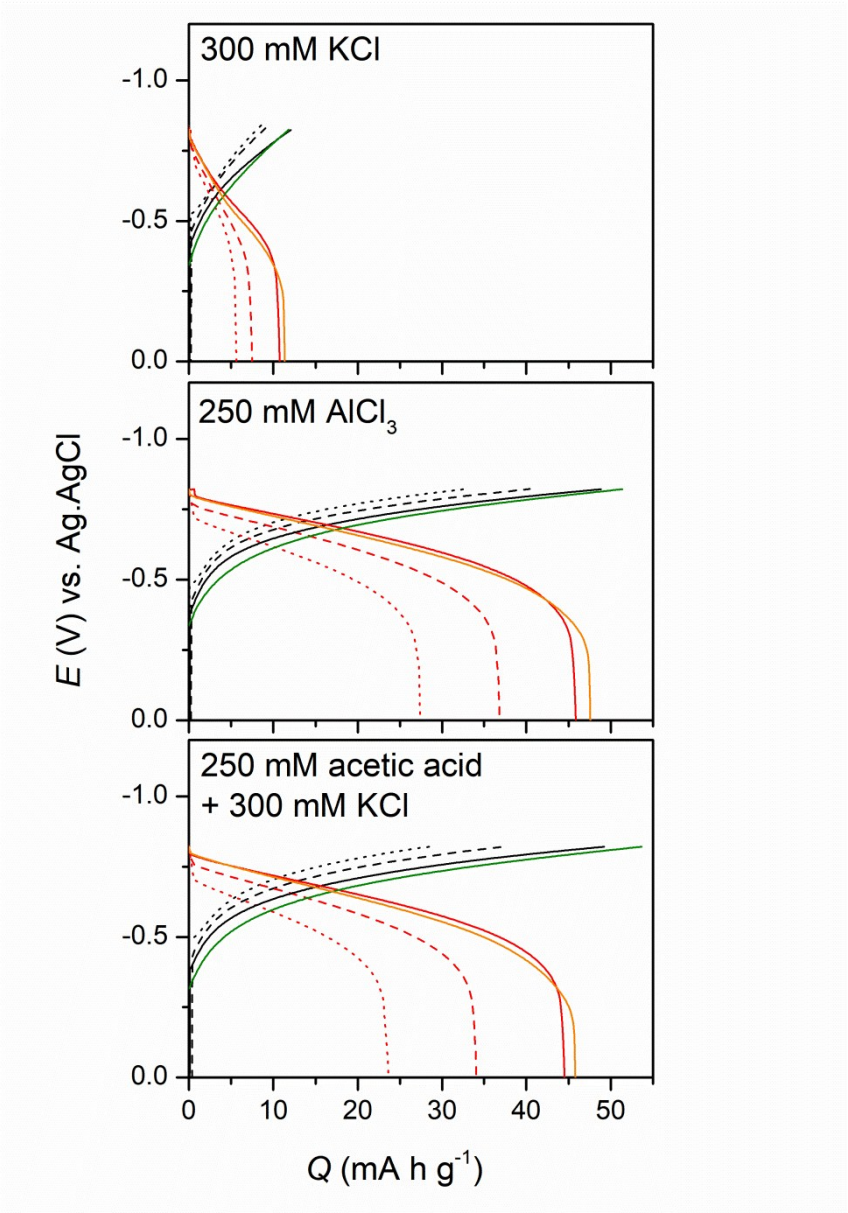

Figure S4. Galvanostatic charging (black and green) and discharging (red and orange) curves recorded at GLAD-TiO_2 electrodes in an aqueous electrolyte adjusted to pH 3.0 and containing (top) 0.3 M KCl, (middle) 0.25 M $AlCl_3$, and (bottom) 0.25 M acetic acid + 0.3 M KCl. The dotted and dashed lines correspond to the charging and discharging curves recorded at a GLAD-TiO_2/TiO_2/ITO electrode, while the plain lines are those obtained at a GLAD-TiO_2/Ti electrode. The applied current density was fixed to (red dotted lines) 2 mA/cm², (red dashed lines) 1 mA/cm², (red and black solid lines) 0.4 mA/cm², and (orange and green solid lines) 0.2 mA/cm² which are equivalent to rates of 48, 24, 10 and 5 C (assuming for TiO_2 a maximal theoretical capacity of 166 mA·h·g^{-1}). The cut-off potential values were -0.82 V and 0.0 V (*vs.* Ag/AgCl) for the charge and discharge curves, respectively.

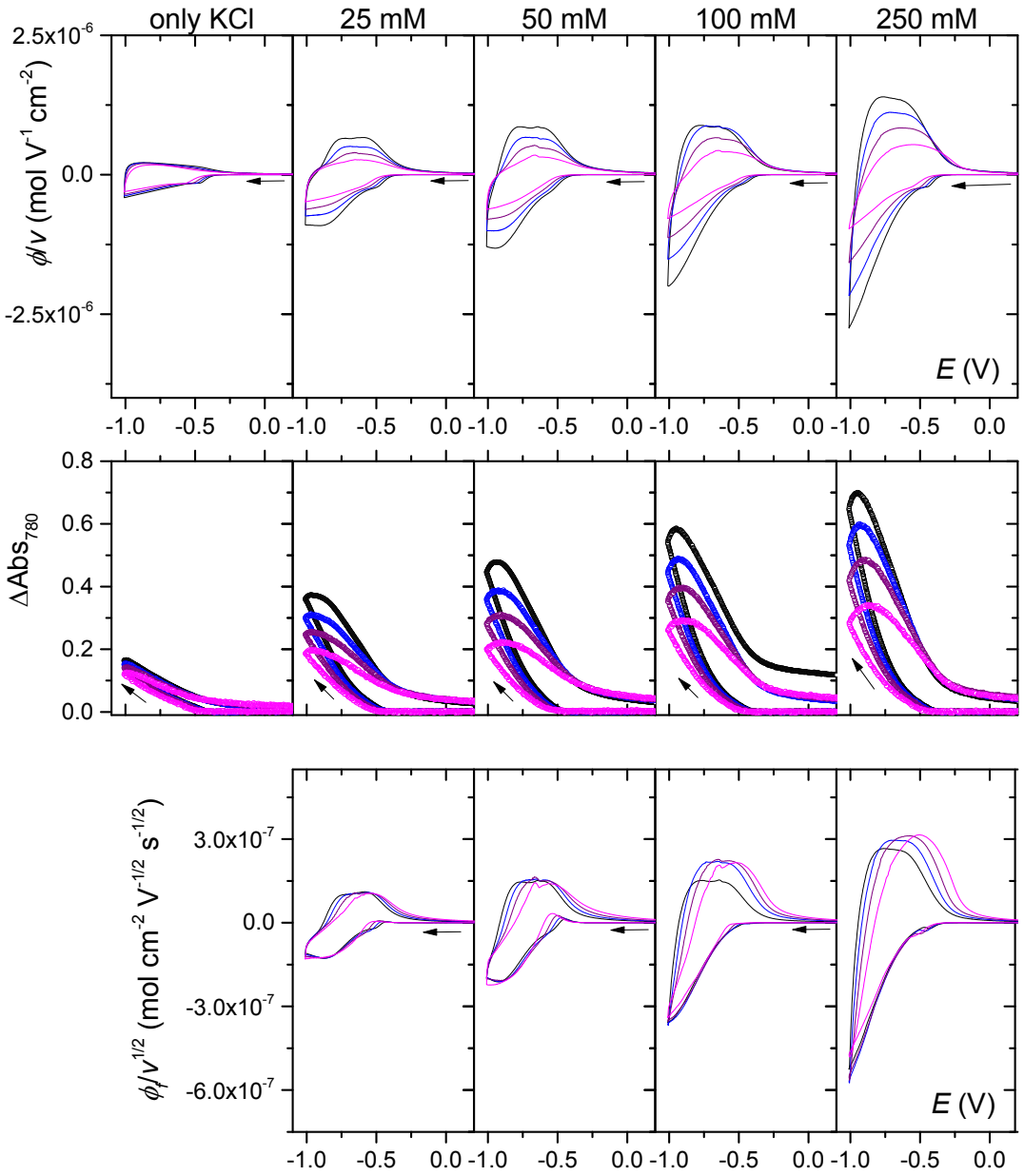

Figure S5. (Top) Cyclic voltammograms and (middle) cyclic voltabsorptograms (at 780 nm) recorded at a GLAD-TiO_2/TiO_2/ITO electrode in different aqueous electrolyte solutions (adjusted to pH 3.0) containing 0.3 M KCl and increasing concentrations of acetic acid (from left to right: 0, 25, 50, 100, and 250 mM). Currents are converted to flux density normalised to the scan rate. The scan rate was (black) 50, (blue) 100, (violet) 250, and (magenta) 500 mV·s^{-1}. (Bottom) Faradaic current component (corrected from the capacitive current) expressed in flux density and normalized to the square root of the scan rate.

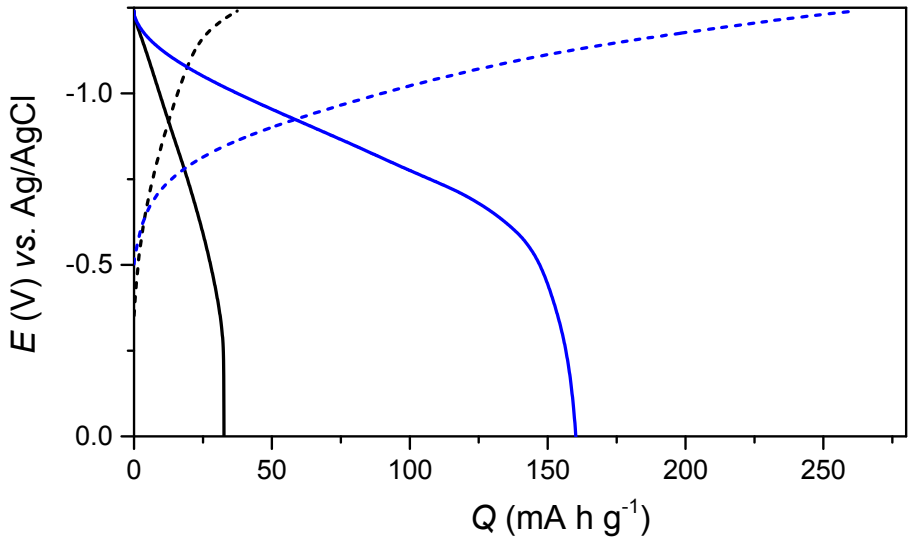

Figure S6. Galvanostatic charging (dashed lines) and discharging (solid lines) curves recorded at a GLAD-TiO_2/Ti electrode immersed in (black lines) a 0.3 M KCl aqueous electrolyte (adjusted to pH 5.0) or (blue lines) a 8 M acetic acid/acetate buffer (pH 5.0). The applied current density was 0.2 mA/cm^2, and the charging/discharging cut-off potentials were -1.24 V and 0 V, respectively.

Table S1. Characteristics of selected cations in aqueous solution including, ionic radii, r_{ion}; distance between ion and surrounding water molecules, $d_{ion\text{-}water}$; number of surrounding water molecules, n, and dissociation constant, pK_a.

Salt	Cation	r_{ion} [S4] (nm)	$d_{ion\text{-}water}$ [S4] (nm)	n [S4]	pK_a [S5]
$AlCl_3$	Al^{3+}	0.053	0.19	6	4.97
LiCl	Li^+	0.069	0.2	4	13.6
$ZnSO_4$	Zn^{2+}	0.075	0.21	6	9
$MnSO_4$	Mn^{2+}	0.083	0.22	6	10.6
KCl	K^+	0.138	0.27	6	14
	H^+	8.7×10^{-7} [S6]			

References

(S1) Kim Y.-S., Kriegel S., Harris K. D., Costentin C., Limoges B., Balland V., Evidencing fast, massive, and reversible H^+ insertion in nanostructured TiO_2 electrodes at neutral pH. Where do protons come from? *J. Phys. Chem. C,* **2017**, *121*, 10325–10335.

(S2) Kim Y.-S., Balland V., Limoges B., Costentin C., Cyclic voltammetry modeling of proton transport effects on redox charge storage in conductive materials: application to a TiO_2 mesoporous film, *Phys. Chem. Chem. Phys.,* **2017**, *19*, 17944–17951.

(S3) Liu L., Yellinek S., Valdinger I., Donval A., Mandler D., Important implications of the electrochemical reduction of ITO. *Electrochim. Acta,* **2015**, *176*, 1374–1381.

(S4) Marcus Y., Ionic radii in aqueous solutions, *Chem. Rev.,* **1988**, *88*, 1475–1498.

(S5) Hawkes S. J., All positive ions give acid solutions in water, *J. Chem. Educ.,* **1996**, *73*, 516-517.

(S6) Beyer A., Maisenbacher L., Matveev A., Pohl R., Khabarova K., Grinin A., Lamour T., Yost D. C., Hänsch T. H., Kolachevsky N., Udem T., The Rydberg constant and proton size from atomic hydrogen, *Science*, **2017**, *358*, 79–85.